Journal of Crystal Growth 117 (1992) 727–731
North-Holland

JOURNAL OF CRYSTAL GROWTH

Nonlinear Zeeman effect of the Ni^{3+} centre in ZnO

P. Thurian, R. Heitz, A. Hoffmann and I. Broser

Institut für Festkörperphysik, Technische Universität, Berlin, Hardenbergstrasse 36, D-W-1000 Berlin 12, Germany

The optical properties of ZnO crystals doped with different enriched nickel isotopes are investigated. Exciting these crystals with photon energies above the excitonic bandgap, a structured luminescence band at 0.76 eV occurs. A nickel isotope splitting in the order of 13.5 μeV/nucleon for the zero phonon lines is resolved. From this isotope effect in accordance with temperature dependent Zeeman-measurements, the luminescence is attributed to the $^4T_2-{}^4A_2(F)$ transition of the Ni^{3+} centre. The zero field splittings of 0.69 meV in the excited and 0.73 meV in the ground state, respectively, are small compared to the Zeeman splitting above $B = 6$ T. Thus the Zeeman behaviour of the centre is studied in both weak and strong magnetic fields. We determine $g = 2.15$ for the $^4A_2$ ground state. For $H \perp c$ the Zeeman splitting is nonlinear, indicating a term interaction.

1. Introduction

The optical and electrical properties of II–VI semiconductors are strongly influenced by the incorporation of nickel. Thereby, the amphoteric character of the Ni centre is important. It is stable in the three different charge states Ni^+ (d^9), Ni^{2+} (d^8) and Ni^{3+} (d^7) [1–3]. Whereas the optical properties of Ni^+ and Ni^{2+} are well known in II–VI compounds, only rare data about Ni^{3+} exist [4]. In nickel-doped ZnO crystals, a luminescence band at 0.76 eV occurs and has been tentatively attributed to a Ni^{3+} transition [5]. The purpose of this paper is to give a detailed analysis of the 0.76 eV luminescence band with temperature dependent magneto-optical spectroscopy to determine the chemical nature, the charge state and the electronic fine-structure of the impurity.

2. Experimental results

The principal doping procedure and the experimental setup are described elsewhere [6]. Our ZnO crystals are doped with natural $^{58/60}Ni$ and the enriched nickel isotopes ^{62}Ni and ^{64}Ni in the ppm range. They display the well-known Ni^{2+} absorption spectra. Exciting these crystals with photon energies above 3.35 eV, a luminescence band at 0.76 eV occurs.

2.1. Fine-structure

The zero phonon line (ZPL) region of the emission is shown in fig. 1. Applying high resolution spectroscopy for ZnO crystals which were

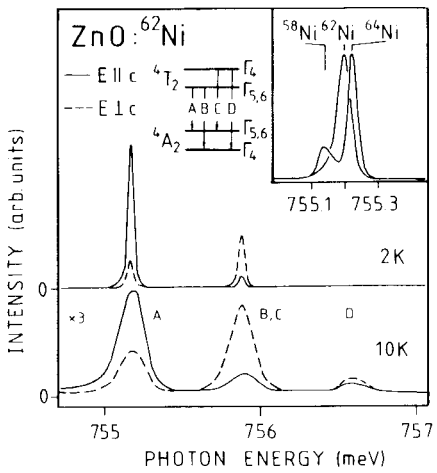

Fig. 1. Polarized ZPL region of the Ni^{3+} centre for $T = 2$ K and $T = 10$ K for ZnO:^{62}Ni and the corresponding fine-structure of the $^4T_2$ and $^4A_2$ states. The insert shows the isotope splitting of emission line A for ZnO:$^{58/60}Ni$, ^{62}Ni and ^{64}Ni doped crystals.

doped with different enriched Ni isotopes, an isotope splitting for the ZPL in the order of 13.5 μeV/nucleon is resolved (see insert in fig. 1). The isotope splitting is positive, i.e., the ZPL of the heavier isotope has a greater ZPL energy. Thus nickel ions participate at the 0.76 eV luminescence band. The emission cannot be a Ni^{2+} transition, since their photon energy excludes a Ni^{2+} transition [1,7]. Exciting the crystal with a photon energy of 3.8 eV at 2 K, the decay time is 350 ± 60 μs, indicating a dipole forbidden transition. Therefore Ni^{+} can also be excluded. We attribute the 0.76 eV luminescence band to the inner $^4T_2$–$^4A_2$(F) transition of the Ni^{3+} centre, which is proved by the Zeeman measurements described below. For $T = 2$ K, the two polarized ZPLs A (755.22 meV ($E \parallel c$)) and B (755.95 meV ($E \perp c$)) are interpreted as $\Gamma_{5,6}(^4T_2)$–$\Gamma_{5,6}(^4A_2)$ (F) and $\Gamma_{5,6}(^4T_2)$–$\Gamma_4(^4A_2)$ (F) transitions of the Ni^{3+} ion (fig. 1). Above $T = 4.2$ K, a hot line (D) at 756.64 meV occurs. With increasing temperature, the two high energetic lines D and (C,B) increase in intensity compared to the low energy ZPL A.

This behaviour can be explained if there is a zero field splitting (ZFS) of 0.73 meV and 0.69 meV in the $^4A_2$ ground state and the $^4T_2$ excited states, respectively. Therefore, the transitions B ($\Gamma_{5,6}(^4T_2)$–$\Gamma_4(^4A_2)$) and C ($\Gamma_4(^4T_2)$–$\Gamma_{5,6}(^4A_2)$) are degenerated in energy at 755.9 meV (fig. 1). Above $T = 30$ K, the ZPLs have vanished, only a broad phonon sideband remains.

2.2. Excitation

Fig. 2 shows the polarized excitation spectra of the Ni^{3+} emission in the band edge region of the ZnO host crystal. The excitation for $E \perp c$ begins just below the excitonic bandgap at 3.350 eV. In the energy range of the free A exciton a maximum of the excitation efficiency occur, whereas for the B and C excitons minima are seen. For energies above $E = 3.5$ eV the excitation of the Ni^{3+} luminescence remains constant.

2.3. Zeeman-measurements

Fig. 3 shows the Zeeman pattern of the ZPL region at $T = 2$ K and $T = 4.2$ K for $H \perp c$ and

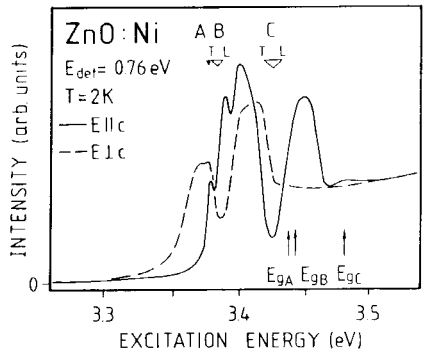

Fig. 2. Excitation spectra of the $^4T_2$–$^4A_2$(F) transition of the Ni^{3+} centre in ZnO at $T = 2$ K.

$H \parallel c$. These given results are obtained with a ^{64}Ni-doped ZnO crystal. For a ^{62}Ni- or a ^{58}Ni-doped crystal the ZPLs are only shifted according to the isotope effect mentioned above. The splitting is linear for $H \parallel c$, whereas in the configuration $H \perp c$ the Zeeman behaviour between $B = 2$–5 T is nonlinear. The temperature dependence of the intensity ratios of the ZPLs in the magnetic

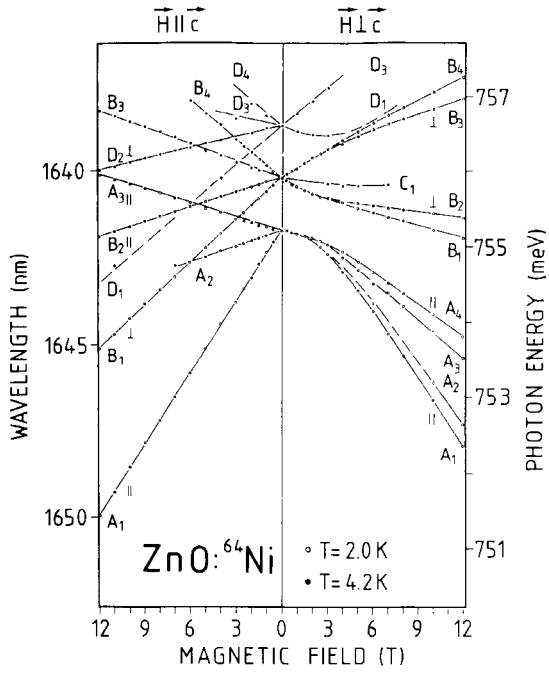

Fig. 3. Zeeman pattern of the ZPL region for $H \parallel c$ and $H \perp c$ for ZnO:^{64}Ni. The fourfold splitting of the $^4A_2$(F) ground state is indicated by the emission lines (B_2, B_1, A_3, A_1) ($H \parallel c$) and (B_3, B_1, A_3, A_1) ($H \perp c$).

field allow us to distinguish between the splittings of the ground and excited states.

2.4. $H \| c$

The emission lines A_1, A_3, B_1 and B_2 are seen for $T = 2$ K. Their intensity ratios are temperature independent in the whole magnetic field range. Thus, the initial state of this luminescence lines is the lowest component of the $^4T_2$ state. Therefore, the energy differences between (A_1, A_3) and (B_1, B_2) represent the splittings of the $\Gamma_{5,6}(^4A_2)$ and the $\Gamma_4(^4A_2)$ ground states, respectively.

The g-values are $g(\Gamma_{5,6}(^4A_2)) = 6.45 \pm 0.02$ and $g(\Gamma_4(^4A_2)) = 2.15 \pm 0.02$. Thermalization occurs for the emission lines A_2, B_3 and B_4, therefore, the energy differences between the emission lines (A_1, A_2), (B_1, B_3) and (B_2, B_4) represent the Zeeman splitting of the excited $\Gamma_{5,6}(^4T_2)$ state. We obtain $g(\Gamma_{5,6}(^4T_2)) = 4.55 \pm 0.04$. The emission lines D_1–D_4 are only seen for $T > 4.2$ K. Their initial states are the two components of the $\Gamma_4(^4T_2)$ state. The energy difference between (D_1, D_3) and (D_2, D_4) represents the splitting of the $\Gamma_4(^4T_2)$ state, the g-value is $g(\Gamma_4(^4T_2) = 3.86 \pm 0.06$.

2.5. $H \perp c$

The emission lines A_1, A_3, B_1 and B_3 are seen for $T = 2$ K, and their intensity ratios are temperature independent in the whole magnetic field range. Therefore, the energy differences between (A_1, A_3) and (B_1, B_3) represent the splitting of the $\Gamma_{5,6}(^4A_2)$ and the $\Gamma_4(^4A_2)$ ground states. The intensity ratios between the emission lines (A_2, A_1), (A_4, A_3), (B_2, B_1) and (B_4, B_3) increase with temperature. Thus, their energy differences are the Zeeman splitting of the $\Gamma_{5,6}(^4T_2)$ excited state. For $B \to 0$ T, $g(\Gamma_{5,6})$ is zero. The emission lines C_1, D_1 and D_3 occur for $T > 4.2$ K. Their initial state originates from the $\Gamma_4(^4T_2)$ state.

3. Discussion

The energetic positions and the g-values of the zero field states are summarized in table 1. The observed Zeeman behaviour of the ground state excludes Ni^{2+} as luminescence centre. A comparison of our data with ESR measurements for $ZnO:Ni^{3+}$ [4] (see table 1) yields excellent agreement for the $^4A_2(F)$ ground state g-values, indicating Ni^{3+} as luminescence centre. As no corresponding Ni^{3+} absorption or ESR signals are observed for unilluminated ZnO crystals, the Ni^{3+} is created by a charge transfer process of Ni^{2+}. The main excitation process for the Ni^{3+} centre is the creation of free carriers and the capture of the hole by the Ni^{2+} leading to the transient Ni^{3+} state. The threshold energy is thereby in the order of 3.350 eV. The structured excitation in the excitonic range leads to the conclusion that different energy transfer processes between the deep impurity and the excitons take place [8]. The time constant leading to equilibrium under excitation is given by the luminescence rise time which is in the order of 210 ± 60 μs. The luminescence decay time for the $^4T_2$–$^4A_2$ transition is 350 μs and is in the order of the reported data for the $^3T_2$–$^3A_2$ transition in $ZnS:V^{3+}$ (280 μs) [9]. The crystal field parameter $10Dq$ of the Ni^{3+} (6090 cm^{-1}) is larger than the corresponding one

Table 1
The energy differences, the observed magneto-optical g-values for $B < 2$ T and $B > 6$ T and the ESR g-values of the Ni^{3+} centre in $ZnO:^{64}Ni$.

		E (meV)	$g_\parallel$		$g'_\perp$		
			Opt.	ESR [4]	Opt. $B < 1$ T	ESR [4]	Opt. $B > 5$ T
$^4T_2$	Γ_4	756.638 ± 0.01	3.86 ± 0.04				4.38 ± 0.06
	Γ_5 Γ_6	755.947 ± 0.01	4.55 ± 0.04		0		4.38 ± 0.06
$^4A_2$	Γ_5 Γ_6	0.725 ± 0.01	6.45 ± 0.02		0		4.32 ± 0.04
	Γ_4	0	2.15 ± 0.02	2.1426	4.4 ± 0.2	4.3179	4.32 ± 0.04

of $ZnO:Co^{2+}$ (4500 cm^{-1} [10]. This can be understood qualitatively by considering the effects of the charge of the ion. The greater the charge, the closer the ligands will be pulled by the electrostatic force, thus a stronger crystalline field and a larger value of $10Dq$ will result. The fact that the polarization selection rules are fulfilled predominantly, but not rigorously, can be caused by mixing of the excited $\Gamma_{5,6}$ and Γ_4 states by internal strains or by a Jahn–Teller effect in the excited $^4T_2$ state. The positive isotope effect is caused by a stronger mass dependence in the ground state and calls for a Jahn–Teller effect in the excited state. A detailed description of isotope splittings and the Jahn–Teller effect is given in ref. [3]. The level scheme for the fine-structure of the $^4T_2(F)$–$^4A_2(F)$ transition shown in the insert of fig. 1 agrees with the corresponding Co^{2+} term scheme in ZnO [10]. The ZFS of the $^4A_2$ ground state (table 1), which is caused by the spin–orbit interaction and the trigonal crystal field described by the parameter 2D, is positive.

3.1. Zeeman behaviour

In contrast to convenient ESR experiments, the Zeeman behaviour of the centre in the whole magnetic field range is observed and additional information is obtained.

3.2. $H \parallel c$

For $H \parallel c$, the spin quantum number S_z remains a good quantum number and the Γ_4 $(\pm 1/2)$ state splits into a Γ_4 $(+1/2)$ and a Γ_5 $(-1/2)$ state, whereas the $\Gamma_{5,6}$ $(\pm 3/2)$ state splits into two Γ_6 states respectively. Thus, no term interaction occurs and the Zeeman behaviour is linear in the whole magnetic field range. The g-value of $g = 2.15$ is the g-value of the whole spinlike $^4A_2$ ground state since $3g(\Gamma_4(^4A_2)) = g(\Gamma_{5,6}(^4A_2))$.

3.3. $H \perp c$

Both $\Gamma_{5,6}$ and Γ_4 states split into a Γ_3 and a Γ_4 state if a magnetic field with $H \perp c$ is applied. Since for $H \perp c$ the Zeeman and the c_{3v} operator did not commutate anymore, a mixing of states with the same symmetry by the magnetic field occurs in the transition region from weak to strong magnetic fields causing the nonlinear Zeeman behaviour. An adequate description is given by MacFarlane [11]. If we assume a mixing of states via the magnetic field, the energy difference ΔE between the centres of gravity of the $\Gamma_{5,6}$ and the Γ_4 states is given by eq. (1):

$$\Delta E = \mu_B B G_\perp = \left[(2D)^2 + (g'_\perp \mu_B B)^2\right]^{1/2}, \quad (1)$$

where 2D is the zero field splitting $g'_\perp$ the effective g-value and $G_\perp$ the "nonlinear g-value".

For $B > 10$ T, we get $G_\perp \to g'_\perp$, in good agreement with our strong field g-values. The observed Zeeman behaviour of the centre can be fitted with eq. (1) and the g-values listed in table 1. The splitting of the $\Gamma_{5,6}$ states for $H \perp c$ is only caused by mixing of states from the Γ_4 levels. For small mixing, i.e., $B \to 0$ T, $g_\perp(\Gamma_{5,6}) = 0$ is expected in good agreement with our observations.

3.4. Angular Zeeman dependence

Fig. 4 shows the angular Zeeman dependence of the ZPL at $B = 12$ T for $T = 2$ K and $T = 4.2$

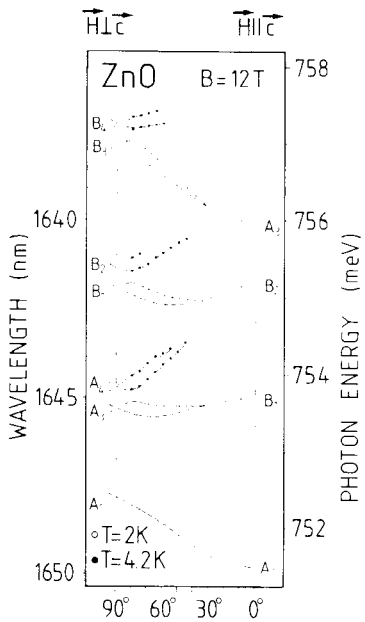

Fig. 4. Angular Zeeman dependence of the ZPL region at $B = 12$ T for $ZnO:^{64}Ni$. The doubling of all ZPLs between $\Theta = 85°$–$40°$ is seen, indicating the two different cation sites in the wurtzite host crystal.

K. While rotating the crystal c-axis from $H \perp c$ to $H \parallel c$, a doubling of all ZPLs is resolved for $\Theta = 85°–40°$ which is not seen for $H \parallel c$ and $H \perp c$. The splitting is the same for all emission line pairs and their intensity ratio is temperature independent. The absence of thermalization between the ZPL pairs leads to the conclusion that there are two inequivalent Ni^{3+} centres.

In a wurtzite crystal two inequivalent lattice sites exist, related by a 60° rotation. These two sites are only equivalent for $H \parallel c$ and $H \perp c$, but are generally different due to the cubic terms in the Zeeman operator. A similar behaviour is known from ESR measurements of Fe^{3+} in ZnO [12]; however, our work presents the first magneto-optical measurements of such a behaviour.

4. Conclusion

In this paper we report a detailed magneto-optical investigation of the $^4T_2$–$^4A_2$(F) transition of the Ni^{3+} centre in ZnO for the first time. The Ni^{3+} centre is created by a charge transfer process of the Ni^{2+} centre. The energy threshold for this process is in the order of 3.350 eV. An isotope splitting of 13.5 μeV/nucleon is observed. The order of ZFS in both $^4A_2$ ground and excited $^4T_2$ states enabled investigations in the weak and strong magnetic field case. The Zeeman behaviour has a model-like character for other d^7 systems in trigonal hosts. The angular Zeeman behaviour allows one to distinguish between the two inequivalent Ni^{3+} sites in ZnO.

Acknowledgements

The authors wish to thank Professor E. Mollwo and Professor G. Heiland for supplying the pure ZnO crystals and E. Birkicht for the doping procedure. This work was partly supported by the Deutsche Forschungsgemeinschaft.

References

[1] H.A. Weakliem, J. Chem. Phys. 36 (1962) 2117.
[2] R.K. Watts, Phys. Rev. 188 (1969) 568.
[3] A. Hoffmann and U. Scherz, J. Crystal Growth 101 (1990) 385.
[4] W.C. Holten, J. Schneider and T.L. Estle, Phys. Rev. 133 (1964) A1638.
[5] H.J. Schulz and M. Thiede, Phys. Rev. 35 (1987) 18.
[6] I. Broser, A. Hoffmann, R. Germer, R. Broser and E. Birkicht, Phys. Rev. B33 (1986) 8196.
[7] U. Kaufmann and P. Koidl, J. Phys. C7 (1974) 791.
[8] K.H. Pantke, H. Over and I. Broser, J. Luminescence 45 (1990) 232.
[9] G. Goetz and H.J. Schulz, J. Luminescence 40/41 (1988) 415.
[10] P. Koidl, Phys. Rev. B15 (1977) 2493.
[11] R.M. MacFarlane, Phys. Rev. B1 (1970) 989.
[12] R.M. Walsh and L.W. Rupp, Phys. Rev. 126 (1962) 952.